Article

Structural Influence on Raman Scattering of a New C Thin Film Prepared by AAO Template with the Method of Pressure Difference

Luo Zhixun, and Fang Yan

J. Comb. Chem., **2006**, 8 (4), 500-504• DOI: 10.1021/cc050140a • Publication Date (Web): 03 May 2006

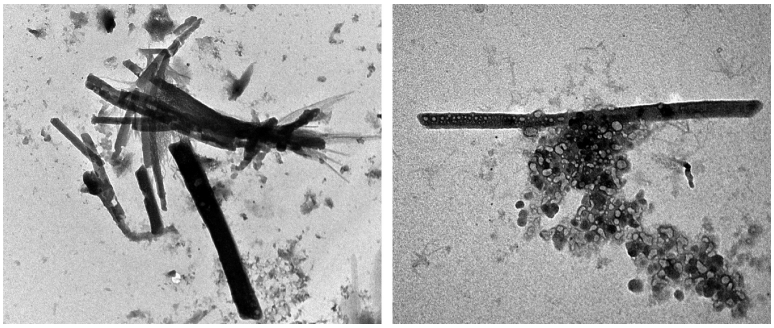

Structural Influence on Raman Scattering of a New C_{60} Thin Film Prepared by AAO Template with the Method of Pressure Difference

Luo Zhixun and Fang Yan*

Beijing Key Lab for Nano-photonics and Nano-structure, Department of Physics, Capital Normal University, Beijing 100037, P. R. China

Received October 13, 2005

An anodic aluminum oxide (AAO) template is prepared by anodizing aluminum in oxalic acid solution. C_{60} crystals were grown, using the pressure difference method, in the pores of the template, representing a brushlike thin film layer with a honeycomb boundary structure in one side and nail arrays in the other side. Different Raman spectra of the C_{60} thin film from the both sides are presented, which indicate the different uniformly ordered structure character and the interface behavior of the C_{60} film on the surface with C_{60} crystals in the AAO nanopores. On the basis of energy and group theory, the strengthening of the Raman intensity and the broadening of Raman modes may imply that more transition spectral lines between vibration or rotation energy levels of C_{60} molecules were excited and detected.

I. Introduction

Since the discovery of a method to synthesize a large amount of C_{60},[1] much work has been done to clarify the physical and chemical properties of solid C_{60}, as well as C_{60} molecules. The various natures of an isolated C_{60} molecule are retained in a crystal because the C_{60} crystal is a molecular crystal in which quasispherical C_{60} molecules are attracted by weak intermolecular forces. In addition, a C_{60} fullerene is a kind of semiconductor material with strong electron-acceptor ability. When it intermingles with other crystal, semiconductor, or metal materials or organizes a thin film on these materials, the charge-transfer becomes very active, which results in unique interface characteristics and has been regarded as a new generation of latent applications in light-detector and cell-battery devices.

Recently with the upsurge of nanotechnology, many kinds of ordered nanostructure materials, as their unique characters, begin to be widely applied in electronics, optics, machines, druggery franchise, and biochemistry.[2−8] There are many methods of synthesizing nanomaterials, including physical and chemical methods. The chemical method usually goes from the bottom to the top; in other words, the nanomaterials are prepared by proper chemical interactions based on the molecules and atoms with simple equipment and mild conditions, and it can be used to make some materials with complex and special configurations cannot be prepared by usual physical methods. For example, the ordered nanodot, nanotube, and nanowire arrays, prepared by templates because of their physical properties, present an entirely new appearance and wide recognition. On the basis of the space restrictions of the template, the bulk, shape, and configuration can be controlled by the design of the template itself in advance.

* Corresponding author. E-mail: lzxnps@126.com.

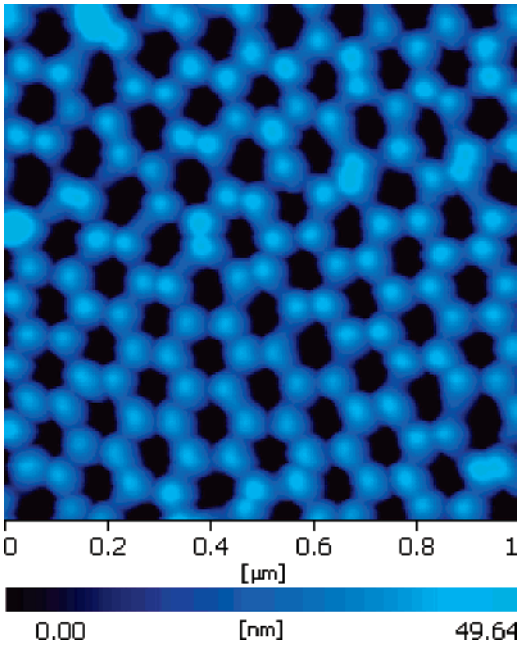

Figure 1. AFM of the AAO template (the front side).

An anodic aluminum oxide (AAO) template,[9−15] which has a hexagonally ordered pore array, is one of the most ideal templates used to synthesize nanometer array materials, as in nanocopy. The high-purity aluminum foil, through anodicoxidation treatment in acid solution, can spontaneously form the pellumina which is typically a self-organizing ordered structure. Because of the uniform aperture of template, the materials prepared by it also keep aperture uniformity and single dispersing, and it is easy to separate the nanotubes or nanofibers from the templates. In fact, templates can prepare not only the tubal or wirelike materials but also the brushlike materials.

Raman spectroscopy, with no damage to the samples, has played an important role in revealing information on the C_{60}

10.1021/cc050140a CCC: $33.50
Published on Web 05/03/2006

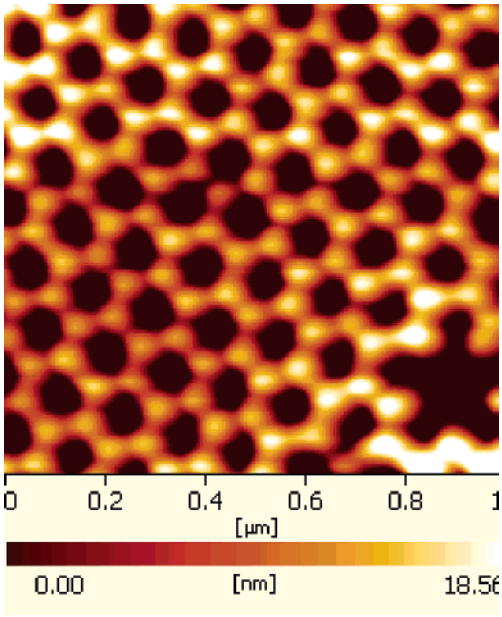

Figure 2. AFM of AAO the template (the backside).

fullerene, including these nanomaterials. In this paper, a series of AAO templates with uniformly distributed pores were prepared, and then the C_{60} fullerene was grown in the pores from one side using the pressure differential method; this, in fact, grew into a brushlike thin film with a honeycomb boundary structure on one side and nail arrays on the other side. Raman spectra of the brushlike C_{60} thin film from the both sides are presented, which indicate the differences in the uniformly ordered structure character and the interfacial behavior between the C_{60} film on the surface and the C_{60} crystals in the AAO nanopores. On the basis of energy and group theory, the broadening of the Raman modes may imply that more transition spectral lines between the vibration or rotation energy levels of the C_{60} molecules were detected and demonstrated.

II. Experiment

AAO templates were prepared according to Masuda.[2] Aluminum foil (99.99%) was put into acetone and vibrated in an ultrasonic cleaning cell to remove the grease on the surface; then it was polished in perchloric acid. The electrochemical anode oxidation action occurred in oxalic acid with a voltage of 50 V. A $CuCl_2$ solution was used to peel off the Al base, and phosphoric acid was for enlarging the pores.

Before the AAO template was taken away from the device, we took the bottles containing the C_{60}/CS_2 solution and water, covered them, and carefully inverted the bottles 90° with one bottle upright and the other upside down. The pressure difference was maintained for 3 days. The concentration of the solution of C_{60} is 0.02 M. Raman spectra excited in the near-infrared region were acquired with a FT-Raman spectrometer, a Brucker Model IFS-66 FT-Raman spectrophotometer with a line resolution of 1 cm^{-1}, and a YAG laser operated at 1064 nm was used as the excitation source at 100 mW.

III. Results and Discussion

A. Preparation of Porous AAO Templates. Figure 1 shows the AFM photo of porous AAO template. It can be seen from the figures that the template is arranged with consistent and uniformly distributed pores with almost identical sizes (~70 nm). Figure 2 presents the AFM photo of AAO template from the other side. It more clearly shows the hexagonal pores. It is interesting that the pores are so uniformly assembled. This may be a result of the process of forming an alumina film, a self-assembled course including substitution and oxidation−reduction reactions.

According Keller and Faller, the dissolution and film-forming reactions of metal are associated in the course of anodic oxidation, just as in all the processes of synthetic membranes. The dissolution reaction of metal is named as origination, and the film-forming reaction is named as windup. We conclude the reactions as follows:

$$Al + 3H^+ \rightarrow Al^{3+} + \frac{3}{2}H_2\uparrow \quad (1)$$

$$2Al^{3+} + 3H_2O + 6HC_2O_4^- \rightarrow Al_2O_3 + 6H_2C_2O_4$$

$$2Al^{3+} + xH_2O + yHC_2O_4^- \rightarrow Al(OH)_x + xH^+ \quad (2)$$

Usually, the pores of templates are cylindrical; however, from Figure 1 we can see that these pores present the surface outline of hexagon arrayed cells. This may result from the self-assembled process and the lattice structure itself. As already known, the porous Al_2O_3 film is composed of an undefined structured oxide; the pore elongates to the interface of oxide and metal base, where there is also a layer of compact thin oxide film called barrier layer. With the processes of chemical dissolution and electric assistance to solvency, which acts as the effect from the voltage of anodic-oxidation treatment, to help to the dissolution reaction and benefit the transportation of charges, each pore and its ambient field combined form a thick interstitial texture, as shown in Figure 3.

B. Preparation of the Brushlike Thin Film of C_{60} Fullerene. Figure 4 shows the AFM image of AAO template with mosaic coatings of C_{60} fullerene by pressure difference method. As we can see, it is remarkable that there are so many regular hexagonal cells spread uniformly like a honeycomb. These hexagonal cells join each other with the length of a side up to ~100 nm. In addition, these cells are steady-going and never vary with the pressure or temporal hours. We guess that it may be the result of the border effect of the AAO nanopores itself, so that the film coated on the AAO template also remains the hexagonal border as the solution infiltrates in along the wall of the pores.

Figure 5 presents the profile feature of the brushlike thin film of C_{60} fullerene. It represents a three-dimensional effect in the upper side with a developed incision method from the cross side. Not only the straightness and the uniformity are notable but also that the nail arrays disperse according with the pores presented from the frontpiece. In addition, different from the pores of thin polymer films prepared by track etching, these pores and rods are not inclined or independent and present no interleaving with each other.

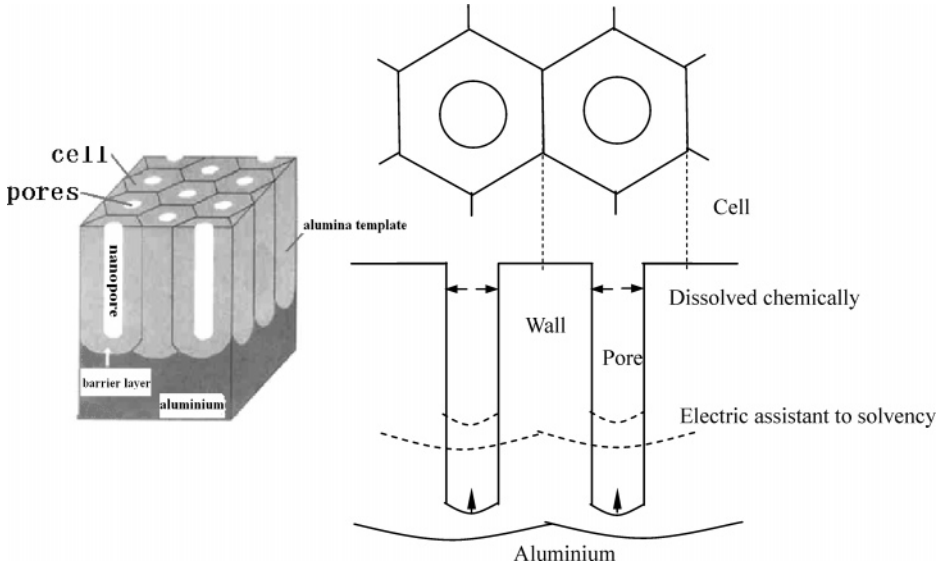

Figure 3. AFM image of the C_{60} thin film on the AAO template.

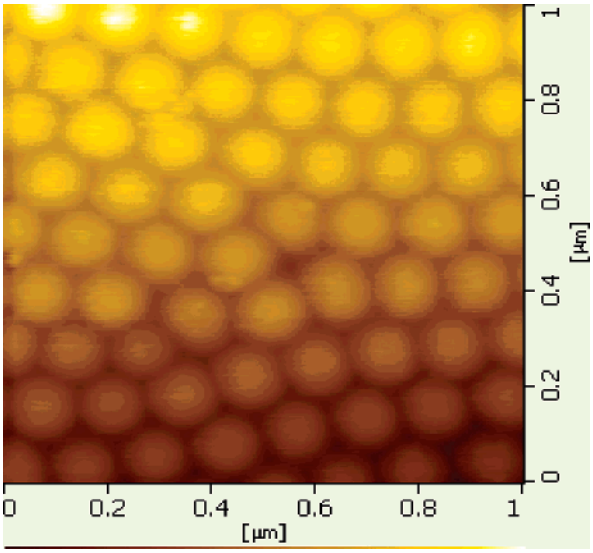

Figure 4. SEM photo of the AAO template filled with C_{60} rods or tubes from the cross side.

Figure 6. presents the AFM image of the AAO−C_{60} thin film from the other side. Here, we cannot find that well-proportioned array of pores. On the contrary, most of these pores are half-filled or blocked. It may be the C_{60} clusters filling in the pores of AAO template, which represents the thin film composed of many brushlike structured cells, as shown in Figure 7.

To show ifC_{60} is filled into the pores, Figure 8 is the lay out of the TEM photo after it was removed from the alumina framework with NaOH solution. Here we can see clearly the rods and tubes, as well as the C_{60} clusters.

Usually, the pore density of AAO template is distributed as

$$\rho_{\text{pore}} = \alpha/(D_{\text{P}} + \beta V)^2 \qquad (3)$$

where α is a constant ($\sim$1.15), D_P is the aperture, β is also a constant correlated to properties of the medium and the temperature, and V is the oxygenation voltage. Since the aperture is a direct ratio to V, the line density of the rod/

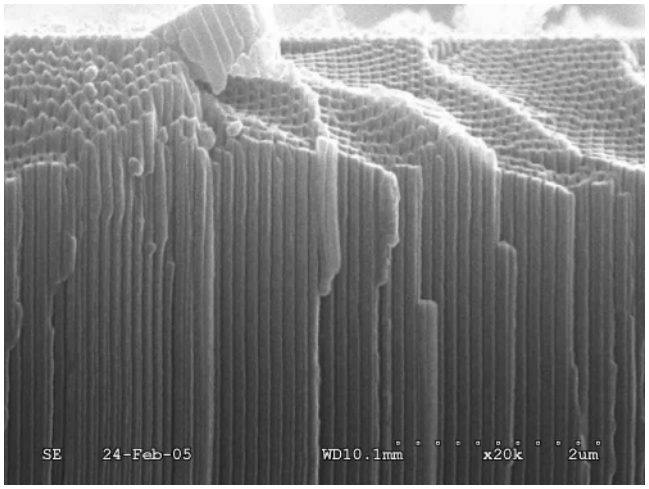

Figure 5. AFM image of the AAO template filled or half-filled with C60 rods or tubes in it pores (from the other side).

tube arrays prepared in the pores decreases with the accretion of the aperture, which brings a large difference to their physical and chemical properties. On the basis of this information, we may control the modification of their properties for the brushlike thin film.

C. Raman Scattering of the C_{60} Thin Film. Figure 9a shows the Raman spectrum of simple AAO template; as can be seen, there are almost no Raman peaks visible. Figure 9b presents the Raman spectrum of C_{60} grown in the pores of AAO with the rod side exposed to the laser. The 10 expected Raman peaks of C_{60} are clearly apparent in the corresponding bands with very good signal-to-noise ratios, especially the three main modes of 272, 497, and 1467 cm^{-1}. Similarly, Figure 9c shows the Raman spectrum of the same C_{60}−AAO film from the film side, and for comparison, Figure 9d shows the Raman spectrum of solid C_{60} powder.

It is interesting that the Raman intensity of solid C_{60} powder is not as strong as that of the brushlike C_{60} film; it is even much weaker than that presented in Figure 9b. In fact, the concentration of C_{60} in the pores of the AAO template is rather less than that of solid powder. But it is obvious that the rods and tubes of C_{60} crystals give much

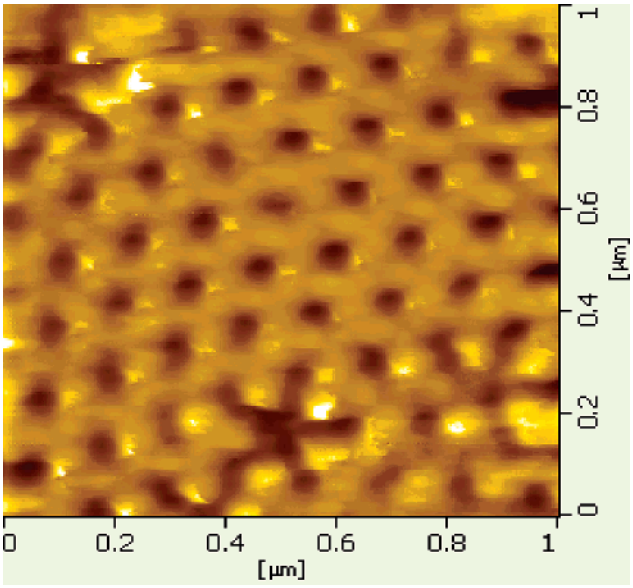

Figure 6. Sketch map of the brushlike thin film of C_{60} with rods or tubes.

better signal-to-noise ratios, as shown in Figure 9b. It is notable that all the Raman modes, no matter in which side, coincide well with the Raman spectrum of solid C_{60}, even without a red or blue shift. But it is different from the surface-enhanced Raman scattering (SERS) of a C_{60} fullerene adsorbed onto a metal substrate where not only were a number of vibrational modes greatly increased but also some additional modes that were forbidden in the Raman spectrum appeared and even split as prediction of group theory.

However, in addition to the strong Raman intensity, most modes are strengthened and broadened, even a shoulder of the 272 cm^{-1} mode can be seen in Figure 9c. Usually the intermolecular vibrational modes strengthen and broaden drastically as the rotational-ordering transition occurs in some situations, such as surface adsorption or temperature increase. According to Hamanaka,[16] the broadening of Raman bands caused by the increase in the inhomogeneity of the intermolecular force fields corresponds to the increase in the orientational disorder of the C_{60} molecules above the phase transition. So we infer that the differences in these Raman spectra may originate from the ordered or unordered structure in both sides of the brushlike thin film of C_{60} fullerene. Because the C_{60} molecules in solid powder are assembled with unordered conditions, as to its high symmetry, the Raman spectrum usually presents rather simple and weak modes in common conditions.

Writing the Raman cross section as

$$\frac{d\sigma}{d\Omega} = \frac{1}{3}k^4\left[\frac{\partial\alpha}{\partial r}\delta r\right]^2 \tag{4}$$

one can grasp that, because of the increase of a specific area exposed to the laser for transparency of AAO template, the ordered structured C_{60} molecules in the nanopores of AAO present a larger scattering cross section.

On the other hand, the total energy of internal motions of molecule is given by

$$E = E_e + E_v + E_r \tag{5}$$

where E_e represents the energy of electron motion, E_v is the energy from the molecular vibrations, and E_r is the energy from rotary movement. When the molecules turn from the state of E'' to E' ($E' < E''$), it leads to electromagnetic radiation

$$\upsilon = \frac{E'' - E'}{h} = \frac{1}{h}[(E_e'' + E_v'' + E_r'') - (E_e' + E_v' + E_v')] = \frac{\Delta E_e}{h} + \frac{\Delta E_v}{h} + \frac{\Delta E_r}{h} = \upsilon_e + \upsilon_v + \upsilon_r \tag{6}$$

As already known, the energy difference of electron motion (ΔE_e) is larger than that of molecular vibrations (ΔE_v), followed by that from rotary movement (ΔE_r), so it is obvious $\upsilon_e > \upsilon_v > \upsilon_r$. When an electron transitions one orbit to another, it results in not only radiant emission or adsorption but also in changes of the electron cloud distribu-

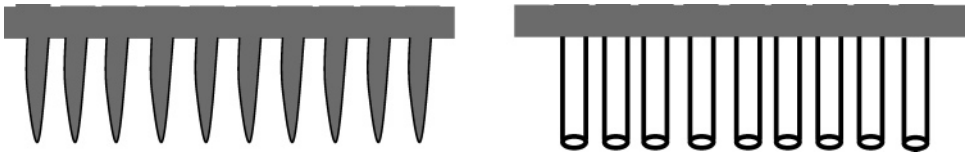

Figure 7. TEM photos of the C_{60} rods or clusters prepared by AAO.

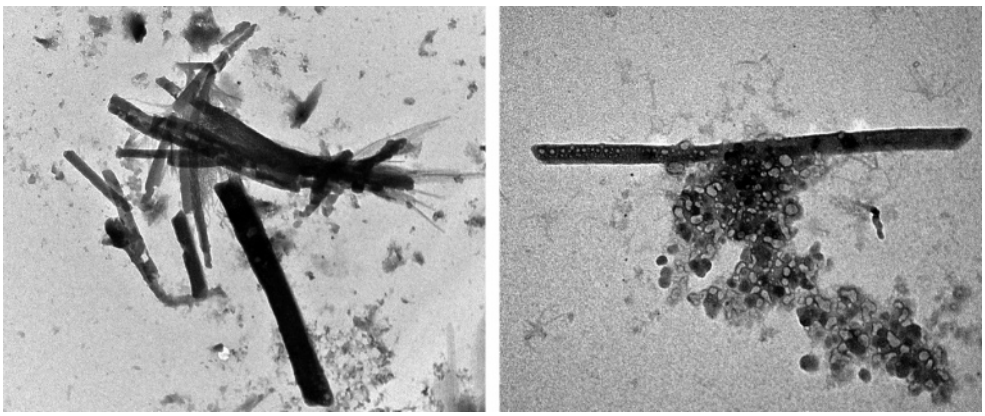

Figure 8. Sketch map of the growth of the regular pores in the AAO template.

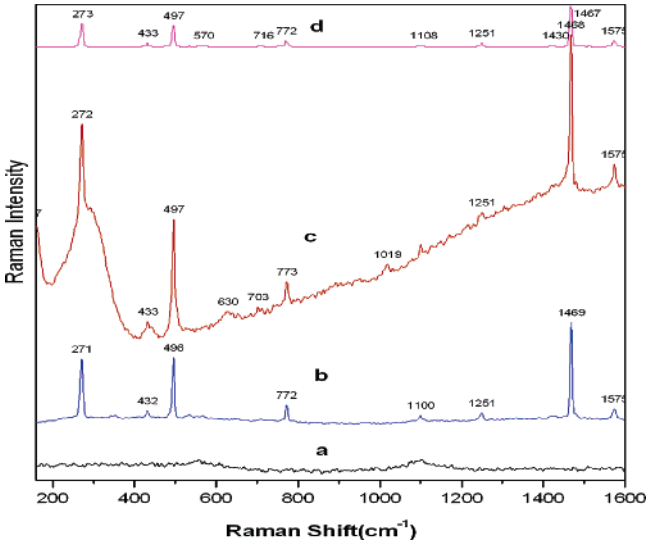

Figure 9. Raman spectrum of the AAO template (a). Raman spectra of C60 grown in the pores of AAO with the brush side (b) and the film side exposed to the laser (c). Raman spectrum of solid C60 (d).

tion and interkernel static force, which may change the cohesion and distance among kernels until a new balance is achieved. Hence, the electron transition of molecules cannot do anything result in the changes of the vibrational state of atoms. And the changes of vibrational state will augment or diminish the rotary inertia which results in the variety of the rotary state. Generally, the electron transition of molecules must bring along the transition between rotational energy level and vibrational level.

In regard to a series of vibrational energy levels and rotational levels corresponding to them, it turns out to be many transition spectral lines closely distributed on both sides of the level at $\upsilon_e + \upsilon_v$ or $\upsilon_e - \upsilon_v$, which represents a continuous spectrum profile but not separate spectral lines. On the basis of this, the broadening of the Raman modes may imply that more transition spectral lines between vibration or rotation energy levels of C_{60} molecules were excited and detected.

IV. Conclusions

An anodic aluminum oxide (AAO) template was prepared by anodizing aluminum in given electrolytes an an oxalic acid solution. With the pressure difference method, the C_{60} fullerene was grown in the pores of the templates; it is a layer of brushlike thin film with a honeycomb-boundary structure in one side and nail arrays in the other side. Since the aperture is a direct ratio to *V*, the line density of the nanorod or nanotube arrays prepared in the pores decreases with the accretion of the aperture, which brings a large differnce to their physical and chemical properties. On the basis of this information, we may control the modification of their properties for the brushlike thin film.

Different Raman spectra of the brushlike C_{60} thin film from both sides are presented, which indicate the different uniformly ordered structure character and the interface behavior of the C_{60} film on the surface with C_{60} crystals in the AAO nanopores. Because of the transparency of AAO template, the ordered structured C_{60} crystal in the AAO nanopores presents a much larger scattering cross section since the specific area exposed to the laser is increased. On the basis of energy and group theory, the broadening of Raman modes may imply that more transition spectral lines between vibration or rotation energy levels of C_{60} molecules were detected and demonstrated.

Acknowledgment. The authors are grateful for the support of this research by the National Natural Science Foundation of China and the Natural Science Foundation of Beijing.

References and Notes

(1) Krätschmer, W.; Lamb, L. D.; Fostiropoulos, K.; Huffman, D. R. *Nature* **1990**, *347*, 354.
(2) Masuda H.; Fukuda, K. *Science* **1995**, *268*, 1466.
(3) Xu, T.; Qi, S.; Zhao, J.; Chen, J. *Acta Phys.−Chim. Sin.* **1996**, *12*, 276.
(4) Wang, G.; Yan, K.-p.; Zhou, C.; Yan, J.-x. *Electron. Compon. Mater.* **2002**, *21*, 27.
(5) Zhurong, K.; Liya, M. *Appl. Sci. Technol.* **2002**, *29*, 52.
(6) Chi, G.; Feng, Z.; Zhao, J.; Yao, S. *Acta Phys.−Chim. Sin.* **2003**, *19*, 177.
(7) Kovtyukhova, N. I.; Martin, B. R.; Mbindyo, J. K. N.; Mallouk, T. E.; Cabassi, M.; Mayer, T. S. *Mater. Eng. C* **2002**, *19*, 255.
(8) Zhou, J.; Dong, P.; Cai, C.; Lin, Z. *Acta Phys.−Chim. Sin.* **2004**, *20*, 1287.
(9) Jessensky, O.; Muller, F.; Gosele U. *Appl. Phys. Lett.* **1998**, *72*, 1173.
(10) Pontifex, G. H.; Zhang, P.; Moskovits, M. *J. Phys. Chem.* **1991**, *95*, 989.
(11) Dmitric Routkevitch, Martin Moskovis. *IEEE Trans. Electron Devices* **1996**, *43*, 1646.
(12) Nishizawa, M.; Menon, V. P.; Martin, C. R. *Science* **1995**, *268*, 5211.
(13) Kyotani T.; Pradhan, B. K.; Tomita A. *Bull. Chem. Soc. Jpn.* **1999**, *72*, 1957.
(14) Laforgue, A.; Simon, P.; Fauvarque, J. *Synth. Met.* **2001**, *123*, 311.
(15) Naoi, K.; Suematsu, S.; Manago, A. *J. Electrochem. Soc.* **2000**, *147*, 420.
(16) Hamanaka, Y.; Norimoto, M.; Nakashima, S.; Hangyo, M. *J. Phys.: Condens. Matter* **1995**, *7*, 9913−9924.

CC050140A